Hydrol. Earth Syst. Sci. Discuss., 11, 6139–6166, 2014
www.hydrol-earth-syst-sci-discuss.net/11/6139/2014/
doi:10.5194/hessd-11-6139-2014

Hydrology and Earth System Sciences Discussions

Open Access

A high-resolution global dataset of topographic index values for use in large-scale hydrological modelling

T. R. Marthews[1], S. J. Dadson[1], B. Lehner[2], S. Abele[1], and N. Gedney[3]

[1]School of Geography and the Environment, University of Oxford, Oxford OX1 3QY, UK
[2]Department of Geography, McGill University, Montreal H3A 0B9, Quebec, Canada
[3]Met. Office, Hadley Centre for Climate Prediction and Research, (JCHMR), Wallingford OX10 8BB, UK

Received: 10 May 2014 – Accepted: 26 May 2014 – Published: 12 June 2014

Correspondence to: T. R. Marthews (toby.marthews@ouce.ox.ac.uk)

Published by Copernicus Publications on behalf of the European Geosciences Union.

Abstract

Modelling land surface water flow is of critical importance for simulating land-surface fluxes, predicting runoff and water table dynamics and for many other applications of Land Surface Models. Many approaches are based on the popular hydrology model TOPMODEL, and the most important parameter of this model is the well-known *topographic index*. Here we present new, high-resolution parameter maps of the topographic index for all ice-free land pixels calculated from hydrologically-conditioned *HydroSHEDS* data sets using the GA2 algorithm. At 15 arcsec resolution, these layers are 4× finer than the resolution of the previously best-available topographic index layers, the Compound Topographic Index of HYDRO1k (CTI). In terms of the largest river catchments occurring on each continent, we found that in comparison to our revised values, CTI values were up to 20 % higher in e.g. the Amazon. We found the highest catchment means were for the Murray-Darling and Nelson-Saskatchewan rather than for the Amazon and St. Lawrence as found from the CTI. We believe these new index layers represent the most robust existing global-scale topographic index values and hope that they will be widely used in land surface modelling applications in the future.

1 Introduction

Land Surface Models (LSMs) are widely used for predicting the effects of global climate change on vegetation and land surface temperature (Prentice et al., 2007; IPCC, 2013). However, the simulation of hydrological dynamics within LSMs remains relatively simplified because these models are run at grid-box scales (∼ 60–300 km resolution) and the physics they follow is based predominantly on approximations of processes that occur at much finer spatial scales (Ducharne, 2009; Wainwright and Mulligan, 2013). Correctly characterising hydrology is very important because meso-scale/landscape-scale water movements and changes in the water cycle control many effects ranging

HESSD
11, 6139–6166, 2014

from local energy and carbon fluxes to land–atmosphere feedbacks to the climate system to potentially-catastrophic changes in vegetation distributions.

When coupled to atmospheric models, most Land Surface Models (LSMs) can simulate a wide variety of natural and human-modified processes from soil moisture feedbacks on precipitation (Seneviratne et al., 2006, 2010; Coe et al., 2009) and river flow (Gedney et al., 2004, 2006; Clark and Gedney, 2008; Milly et al., 2008; Falloon and Betts, 2010; Sanderson et al., 2012) through to vegetation development and carbon productivity (Prentice et al., 2007; Marthews et al., 2012; IPCC, 2013). Although usually applied at mesoscale resolutions (gridcells of scales 10–100 km, e.g. Harding and Warnaars, 2011), LSMs are increasingly finding applicability at finer resolutions approaching 1–10 km, at which the physics they encapsulate begins to approach the more detailed scales (100–1000 m) typically required in process-based hydrological models or used in catchment-based water resources assessments (cf. Wood et al., 2011, 2012; Beven and Cloke, 2012). A growing body of work has lately emerged using LSMs to produce large-area projections of current and future water resources for use in applications related to climate change impacts assessment (Gedney and Cox, 2003; Gerten et al., 2004; Falloon and Betts, 2010; Wood et al., 2012; Zulkafli et al., 2013; Harding et al., 2013).

Land Surface Models require a representation of surface and subsurface runoff. Models of runoff production used in regional and continental applications typically contain parameterised physics that is based on statistical representations of processes known to operate at finer scales (Ward and Robinson, 2000; Clark and Gedney, 2008). This can lead to inaccurate predictions in data-sparse regions and generally high uncertainty. The large quantity of detailed topographic information now widely available at sub-mesoscale resolutions offers an opportunity to improve the fidelity of large-area simulations of the hydrological cycle, for the benefit of both climate and hydrological models (Dharssi et al., 2009; Wainwright and Mulligan, 2013).

Currently, the most common approach is to use a statistically-generalised runoff production scheme such as TOPMODEL, which partitions runoff from the soil column

HESSD
11, 6139–6166, 2014

into surface and subsurface components (Beven and Kirkby, 1979; Quinn et al., 1991, 1995; Beven, 1997, 2012). One of the most important configurational parameters for TOPMODEL is the well-known *topographic index* (defined in Appendix A), which is widely used in hydrology and terrain-related applications (Ward and Robinson, 2000; Wilson and Gallant, 2000).

The HYDRO1k global values for Compound Topographic Index (CTI) were released by USGS in 2000 (USGS, 2000) and they have since become the most commonly used global ancillary files for topographic index values. HYDRO1k was a great step forward in the development of global hydrological modelling applications: it allowed spatially-explicit hydrological routines to be incoporated in LSMs for the first time and large-scale applications of the TOPMODEL hydrological model to become standard (Beven, 2012). However, because of its relatively coarse resolution (30 arcsec, approximately 1 km at the equator) which limits precise slope calculations, and because it was based on mosaicked elevation data of differing quality over different geographical areas (USGS, 2000), CTI ancillary files are no longer considered ideal and there is a need for improvement.

The limitations of HYDRO1k CTI values become most apparent when considering wetland ares. Wetlands are critical nodes in the Earth System where land–atmosphere fluxes are strongly dependent on seasonal and inter-annual hydrological variability (Coe, 1998; Baker et al., 2009; O'Connor et al., 2010; Dadson et al., 2010). In wetlands, the availability of water introduces important feedbacks on climate via surface fluxes of energy and water and these areas form a key link between the hydrological and carbon cycles (Ward and Robinson, 2000; Gedney et al., 2004; Seneviratne et al., 2006, 2010; Coe et al., 2009; Dadson et al., 2010). Some analyses based on CTI values have persistently overestimated the extent and persistence of tropical wetlands of various types. Notably, simulations using the Earth System Model HadGEM2, which is parameterised using CTI (Collins et al., 2011), predict much larger and more persistent Amazonian wetlands than actually exist according to current surveys (e.g. Lehner and

HESSD
11, 6139–6166, 2014

A high-resolution global dataset of topographic index values

T. R. Marthews et al.

Döll, 2004; Prigent et al., 2007; Junk et al., 2011), which may at least partly be caused by the quality of the HYDRO1k CTI.

In the context of LSMs, the need for high-resolution topographical data across wide spatial domains has recently been highlighted (Lehner et al., 2008; Wood et al., 2011; Lehner and Grill, 2013). With the advent of satellite-based global mapping, notably the Shuttle Radar Topography Mission (SRTM), there has been a significant improvement in the availability of high-resolution datasets with continental coverage, such as in the high-resolution global HydroSHEDS database (Lehner et al., 2008), but unfortunately such datasets have generally not yet been utilised to support large-scale hydrological modelling studies (Wood et al., 2011, 2012).

Responding to the needs for higher-resolution data for use in LSMs, in this study we have three main aims: (1) to calculate the topographic index using the GA2 algorithm based on high-resolution global HydroSHEDS data; (2) to compare our values to the current standard for values of this index (the CTI of HYDRO1k) and (3) to discuss current developments in large-scale hydrological modelling and how models can benefit from higher-resolution parameter maps such as these.

2 Methods

2.1 Topographic index

The topographic index is a parameter that was introduced with the TOPMODEL hydrological model (Beven and Kirkby, 1979; Quinn et al., 1991, 1995; Beven, 1997, 2012). The algorithm required for calculating this index is relatively simple (Appendix A), but it has not previously been applied to generate a global dataset at very high resolution because (1) the index must be calculated from harmonised topographic information, which only became available in the 2000s and (2) Land Surface Models (LSMs) have only recently become sophisticated enough to make use of such a high-quality layer (Prentice et al., 2007).

HESSD
11, 6139–6166, 2014

The HydroSHEDS "hydrologically-conditioned" layers

Grid-based topographic index calculations require a Digital Elevation Model (*DEM*) and we have used the Hydrological data and maps based on SHuttle Elevation Derivatives at multiple Scales (*HydroSHEDS*) *DEM* (Lehner et al., 2008; http://www.hydrosheds.org/). The *HydroSHEDS* database was derived from raw SRTM data at 3 arcsec pixel resolution (approximately 90 m at the equator) through the application of hydrological conditioning in a sequence of correction steps (Lehner, 2013) which resulted in a globally consistent suite of grid layers which were subsequently upscaled to a resolution of 15 arcsec (approx. 450 m at the equator). We acquired the *HydroSHEDS* DEM and also a layer of pre-calculated contributing upstream catchment areas for each 15 arcsec pixel (*UPLAND* in m^2, B. Lehner *unpubl. data* 2013). As of April 2014, *HydroSHEDS* data has only been produced at its highest quality for all land areas south of 60° N, so for areas at higher latitude we substituted the HYDRO1k DEM (disaggregated to 15 arcsec resolution) to provide seamless global grids.

2.2 Generating the ancillary files

Our calculations had to be carried out over domains composed of complete watersheds, so we mosaicked both the *DEM* and *UPLAND* tiles into a global data layer using ArcGIS 10.1 (Esri Inc., Redlands, California). These two input layers were then converted to NetCDF format using *gdal* (OSGF 2011).

Topographic Index values were calculated using the *GA2* algorithm, which is the widely-used *GRIDATB* algorithm with some modifications for use with *HydroSHEDS* data (see Appendix A for details). Resulting index values for the global land surface were then filtered to remove areas for which topographic index values are invalid or meaningless, including lakes and reservoirs (masked out using the Global Lakes and Wetlands Database, Lehner and Döll, 2004), mountain glaciers and ice caps (using the Randolph Glacier Inventory, Pfeffer et al., 2014) and the Greenland ice sheet (using Lewis, 2009).

HESSD
11, 6139–6166, 2014

GA2 was run on the ARCUS server for all continental-scale calculations, a 1344-core computer cluster at the Oxford e-Research Centre (OeRC). Zonal histograms were plotted using ArcGIS 10.1 and subsequent statistics calculated using R (R Development Core Team, 2013).

3 Results

We produced a layer of topographic index (TI) values following the *GA2* algorithm for all ice-free land pixels worldwide. TI values calculated this way are not just relative measures but consistent and comparable between catchments (Appendix A), so we may compare global values:

As expected, TI values are low at ridge-tops (minimal catchment area) and high in valleys (along drainage paths and in zones of water concentration in the landscape, Wilson and Gallant, 2000), yielding a global range of 0.00–25.00 and average of 5.99 (Fig. 2).

Wetter areas of the globe generated generally higher TI values (Fig. 1), although there are many exceptions to this (e.g. in desert areas where high TI values do not correlate with high flow accumulation). Zonal statistics calculated for the various lake and wetland types of the world (as defined by the Global Lakes and Wetlands Database, see Table 2) show that pixels representing rivers had the highest TI values (global mean 8.81 over 0.42×10^6 km^2), but also the highest variance with some river pixels scoring below the global mean for ice-free land outside lakes, reservoirs, wetlands and wetland complexes (global mean 5.88 over 128.99×10^6 km^2). In terms of TI, wetland complexes in Asia (mostly occurring in India and Tibetan China, Table 2) and mires (mostly occurring in boreal Canada and the Russian Federation) were indistinguishable from dry land (Fig. 3), indicating that wetlands in these areas are maintained by factors other than topography.

In comparison to HYDRO1k, the new TI values from *GA2* based on *HydroSHEDS* were higher for river pixels and slightly higher for intermittent wetlands and lakes. TI

HESSD
11, 6139–6166, 2014

values were lower at pixels in tropical swamp forests and inundated forests and also slightly lower in coastal wetlands.

The new TI values from *GA2*/*HydroSHEDS* were in line with HYDRO1k values for Compound Topographic Index (CTI, USGS, 2000) at most global pixels, but in certain areas there were significant divergences. Considering all river catchments larger than 10^6 km^2 in particular (Table 1), CTI values were higher for many basins, most notably the Amazon, Congo, Paraná, Niger and St. Lawrence rivers, in the case of the Amazon as much as 20 % higher than the values from *GA2* (Fig. 4). According to our calculations, the catchments with the highest spatially-averaged TI values were the Murray-Darling, Nelson-Saskatchewan, Nile and Niger (compared to the order Amazon, St. Lawrence, Niger and Nelson under the CTI calculations, although n.b. HYDRO1k's CTI included no estimates for the Murray-Darling, Table 1). Although it might be expected that the size of the Amazon floodplain would be enough to ensure it scored the highest TI, please note that (i) there is no globally consistent correlation between wetland area and TI (Fig. 3) and (ii) because these are spatial averages, the density of wetland within each catchment is more important than the absolute wetland size (and the Nelson-Saskatchewan, for example, is known for a high density of wetland terrain).

Index values are now available at http://www.geog.ox.ac.uk/research/landscape/projects/africanwetlands/africanwetlandsdata.html in NetCDF format and also translated into GeoTIFF format using *gdal* (OSGF 2011), both at 15 arcsec resolution.

4 Discussion

Modelling soil water flow and runoff generation is of critical importance for simulating land-surface fluxes, predicting water table dynamics, wetland inundation and river routing and, at a regional scale, quantifying surface evaporation rates and the growth, transpiration and seasonality of vegetation (Ward and Robinson, 2000; Baker et al., 2009; Dadson et al., 2010; Marthews et al., 2014). Meso-scale or landscape-scale hydrological processes are therefore key elements in modelling land surface–atmosphere

HESSD
11, 6139–6166, 2014

exchange processes and critical to the successful use of coupled LSMs to predict the effects of climate change at larger scales.

The hydrological routines of LSMs have received much attention and undergone steady improvement in recent years (e.g. Gedney and Cox, 2003; Gerten et al., 2004; Dadson and Bell, 2010; Dadson et al., 2010, 2011; Zulkafli et al., 2013; Wood et al., 2011; Wainwright and Mulligan, 2013; MacKellar et al., 2013). However, these meso-scale processes remain generally less well-modelled than processes operating at the finer local-scale (e.g. photosynthesis models) or larger continental-scale (e.g. climate circulation models). Arguably, the development of meso-scale processes has been relatively slow not just because of a lack of complete understanding of the processes involved, but also, more simply, by the limited availability of high-resolution parameter maps for the models concerned (Wood et al., 2011; Wainwright and Mulligan, 2013; Marthews et al., 2014). Because LSMs are now being applied at increasingly high spatial resolution in order to analyse the distribution and movement of water resources, model development is gaining momentum. Large-scale gridded simulations based on high-resolution drivers are now becoming routine, and this has led to an increasingly recognised need for the high-resolution datasets required to drive those simulations (e.g. Wood et al., 2011, 2012; Beven and Cloke, 2012; Castanho et al., 2013).

Since, 2000, there have been many advances in the base data from which topographic index values may be calculated (i.e. improved DEMs such as SRTM, and improved hydrological derivatives such as *HydroSHEDS*). A strong demand has arisen in the land surface modelling community for higher-resolution simulations and there are now even calls for "hyperresolution" global simulations at resolutions down to 100 m (Wood et al., 2011, 2012; Beven and Cloke, 2012). Now is an appropriate time to revisit and update the availability of global hydrological datasets and in this study we have revised and recalculated the widely-used CTI layer of the HYDRO1k database. We have presented new, high-resolution topographic index maps in formats appropriate for use with the latest LSMs.

HESSD
11, 6139–6166, 2014

4.1 High-resolution hydrological modelling

TOPMODEL was originally applied at the scale of small catchments, using pixels less than 50 m × 50 m in extent (Quinn et al., 1991, 1995; Ward and Robinson, 2000; Beven, 2012), with the index values understood to have relative significance only (i.e. similar values calculated in different catchments do not necessarily imply hydrological similarity, see Chappell et al., 2006). There have been many developments from this basic framework over the years (e.g. see Wilson and Gallant, 2000; Hjerdt et al., 2004; Beven, 2012) and this study has likewise taken a novel approach. Notably, we have applied our calculations at continental scales with larger pixels (approximately 450 m × 450 m at the equator), using the resolution correction of Ducharne (2009; also see Moore et al., 1993; Wolock and McCabe, 1995; Clark and Gedney, 2008). Additionally, because our calculations are carried out over complete continental land masses, the index values derived may be considered to be consistent and comparable between catchments.

Although we accept the arguments of Beven and Cloke (2012) that moving to higher-resolution data sets is not the only line of development that should be followed, ultimately we support the ideas of Wood et al. (2011, 2012) that increasing the resolution at which global hydrological simulations are carried out will have many beneficial knock-on effects. Methane production in wetlands, for example, is critically dependent on the level of the water table (Gedney et al., 2004; O'Connor et al., 2010; Pangala et al., 2013), models of which are in turn dependent on accurate representation of the topography, therefore higher resolution simulations involving improved topographic index values should of necessity improve the representation of wetland fluxes of heat, water and trace gases to the atmosphere (Gedney et al., 2004) and overall estimates of methane release.

In this study we have refined the standard topographic index calculations and greatly improved their spatial resolution. We have presented our new maps of topographic index values both by wetland type (using the Global Lakes and Wetlands Database, Lehner and Döll, 2004) and also in terms of the largest river catchments occurring

HESSD
11, 6139–6166, 2014

on each continent, finding that in comparison to our revised values, HYDRO1k's CTI topographic index values were significantly higher in some catchments (Table 1).

4.2 Limitations of the GA2 algorithm

The topographic index is a measure of the relative propensity for soil to become saturated to the surface as a result of local topography (Beven, 2012). We have calculated it using a robust algorithm (GA2) based on the original implementation of these calculations (GRIDATB, Appendix A). Although topographic index values are comparable between different areas, it is important to remain careful when interpreting their meaning in different regions, such as arid vs. humid, or shallow vs. deep soils (i.e. when factors other than topography influence water accumulation in the landscape).

A well-known limitation of topographic index values is that they are not absolute because the maximum value in any particular catchment is dependent on the catchment's area and slope profile. Therefore, when different calculation methods only result in a change of index distribution shape leaving the minimum the same (at 0), as is the case when comparing our TI values from GA2/*HydroSHEDS* vs. the CTI from HYDRO1k (Fig. 4), only a partial validation is possible. Therefore, we cannot state conclusively that our revised values are more correct than those of the CTI from HYDRO1k, but the consistency and rigour of the algorithm used and our closeness to the original GRIDATB implementation as well as the improved *HydroSHEDS* base data used for the calculation lead us to believe that our values are indeed more robust.

A second limitation of our method is that we have used global base elevation data that is not on an equal-area projection. The *HydroSHEDS* data layers are projected using the World Geodetic System (WGS) 1984, i.e. a grid of unrotated cells that are increasingly stretched in the north-south direction as latitude increases. This implies that slopes will be underestimated in east-west directions at higher latitudes as true pixel distances are getting shorter (Appendix A). There is no appropriate method, however, to avoid uncertainty completely in the slope calculations as the underlying SRTM elevation measurements are already unequally spaced, and as there is no commonly agreed

HESSD
11, 6139–6166, 2014

upon slope calculation method (e.g., FD8, MD8, D8). We assume that our calculations of steepest gradients with average pixel distances provide a reasonable compromise to approximate the real slope of each pixel (see Appendix A).

5 Conclusions

In this study we have calculated a new high-resolution, spatially consistent data layer of topographic index values for all ice-free land pixels worldwide based on the hydrologically-conditioned *HydroSHEDS* database (Lehner et al., 2008). These data layers are at four times the resolution of the HYDRO1k compound topographic index layers (USGS, 2000) – actually within the range of "hyperresolution" data as proposed by Wood et al. (2011) – and we believe represent the most robust global-scale calculation of topographic index values that exists to date.

LSMs have now been applied over many years to the problem of explaining and predicting global climate change (Prentice et al., 2007; IPCC, 2013). Recent developments in land-surface modelling and Earth Observation have attempted to incorporate better hydrological understanding into these applications, with a particular focus on a better characterisation of the physical processes that control the water cycle (Coe, 1998; Gedney and Cox, 2003; Coe et al., 2009; Dadson and Bell, 2010; Dadson et al., 2010, 2011; Zulkafli et al., 2013). LSMs are continuing to develop rapidly, but in some ways code development has progressed more quickly than the development of the parameterisations on which code simulations are based (Wainwright and Mulligan, 2013). We have made a significant step to redress this by improving the quality of the widely-used topographic index parameter maps. We hope this will lead to more robust simulations of hydrological dynamics and all the processes that depend on landscape-scale water movements and the water cycle in general.

HESSD
11, 6139–6166, 2014

Title Page
Abstract | Introduction
Conclusions | References
Tables | Figures
◂◂ | ▸▸
◂ | ▸
Back | Close
Full Screen / Esc
Printer-friendly Version
Interactive Discussion

Appendix A: Calculating the topographic index

The *topographic index* is a fundamental parameter of *TOPMODEL*, the TOPography based hydrological MODEL (Kirkby, 1975; Beven and Kirkby, 1979; Quinn et al., 1991, 1995; Beven, 1997, 2012), alternatively known as the *topographic wetness index* (TWI, e.g. Wilson and Gallant, 2000) or the *compound topographic index* (CTI, e.g. USGS, 2000; Evans, 2003). The topographic index is essentially a means of grouping runoff-producing elements in the landscape (Kirkby, 1975; Beven and Kirkby, 1979). Different landscape pixels that have similar topographic index values should be observed to have similar hydrological dynamics (Quinn et al., 1995), allowing for a great simplification of hydrology calculations (Beven, 1997, 2012).

The topographic index is a measure of the relative propensity for the soil at a point to become saturated to the surface, given the area that drains into it A and its local outflow slope β (Beven, 2012; increasing A will tend to increase the accumulation of water, but increasing β will tend to reduce it by increasing gravitational outflow, Quinn et al., 1991). The index is often calculated using an algorithm called *GRIDATB*, originally written in 1983 by K. Beven of the Hydrology Group, University of Lancaster (revised for distribution 1993–1995 by P. Quinn and J. Freer and described in Quinn et al., 1991, 1995).

We calculated topographic index values for each pixel using the *GA2* algorithm, which is a slightly modified version of *GRIDATB* version 95.01 (FORTRAN program *gridatb.f*) written specifically for this study based on the basic loop structure implemented in Buytaert (2011) with some modifications to allow for the use of *HydroSHEDS* data. *GA2* calculates the outflow gradient of each pixel (Fig. A1) and uses precalculated *UPLAND* values from *HydroSHEDS* for the catchment area A of each pixel (corrected for latitudinal projection distortions, B. Lehner *unpubl. data* 2013).

Because of the use of the *HydroSHEDS DEM*, we made three small modifications in *GA2* to the standard *GRIDATB* calculations:

HESSD
11, 6139–6166, 2014

- We applied the correction for *DEM* resolution suggested by Ducharne (2009) to allow calculations to be carried out at continental scales (see below).

- *GRIDATB* used the multiple flow direction algorithm of Quinn et al. (1991, 1995), also known as the FD8 or MD8 routing model (Wolock and McCabe, 1995; Zhao et al., 2009; Lang et al., 2013). However, in *GA2* we instead used a direction-of-steepest-descent model: the Deterministic Eight Node (D8) routing model (Moore et al., 1993; Wolock and McCabe, 1995; Wilson and Gallant, 2000; Zhao et al., 2009). This was for consistency with the *HydroSHEDS* drainage direction approach used to derive *UPLAND* areas in this study, which were calculated using D8.

- The *HydroSHEDS DEM* does not have uniformly-sized grid-cells because of its native geographic projection (WGS84) where pixel dimensions vary with latitude (i.e. the real height of a pixel increasingly exceeds its width towards the poles). Because slope directions are restricted to the eight cardinal and diagonal directions, we account for varying pixel dimensions in our slope calculations by taking an average distance between neighboring pixels (rather than direction-dependent): we approximated *DX* as the square root of the area of each cell (with latitude-corrected pixel areas calculated using the Met. Office Unified Model routine *arealat1.f90* written by T. Oki in 1996; Dadson and Bell, 2010). When away from the equator, this implies that slopes will be slightly overestimated in north-south directions and underestimated in east-west directions.

- Finally, because the value of *dfltsink* is undefined on plains (i.e. areas of no outflow and no inflow, which occur more often when vertical resolution is lower) we followed USGS (2000) and Evans (2003) in applying a minimum of 0.001 to $\tan(\beta')$.

Discussion Paper | Discussion Paper | Discussion Paper | Discussion Paper |
HESSD
11, 6139–6166, 2014
A high-resolution global dataset of topographic index values
T. R. Marthews et al.

A1 Correcting for DEM resolution

A question arises when comparing catchments digitised at different resolutions (e.g. Chappell et al., 2006): how to compare topographic index values calculated from DEMs at different resolutions? Although not part of the original topographic index calculations, it has become accepted that topographic index values as calculated above should be reduced to the "equivalent" value for a 1 m resolution DEM by subtracting $\ln(DX)$ (and restricting the result to be ≥ 0). Although not universally implemented (e.g. neither Evans, 2003 nor Buytaert, 2011 applied it), applying this scale-correction has become standard: e.g. see Ducharne (2009; also see Moore et al., 1993; Wolock and McCabe, 1995; Clark and Gedney, 2008).

A2 Slope calculations

There are many different methods for calculating slopes from DEM data and there is not yet a universally-agreed method (Wilson and Gallant, 2000; Zhao et al., 2009), so the use of D8 above is not an unreasonable modification. Additionally, slope values depend on the resolution of the DEM (being by default higher for smaller resolutions), therefore both the use of D8 (above) and the resolution correction (Ducharne, 2009) modify the slope values in our calculations.

Acknowledgements. This study is part of the project *Changing Land–Atmosphere Feedbacks in Tropical African Wetlands* coordinated by S. J. Dadson (http://www.geog.ox.ac.uk/research/landscape/projects/africanwetlands.html) and funded by the UK Natural Environment Research Council (NERC) and the Centre for Ecology and Hydrology (CEH). N. Gedney is supported by the Joint UK DECC/Defra Met. Office Hadley Centre Climate Programme (GA01101). Unreserved thanks go to the University of Oxford Advanced Research Computing facility (http://www.arc.ox.ac.uk/) and the Oxford e-Research Centre (http://www.oerc.ox.ac.uk/) for their assistance and the use of the HAL and ARCUS servers for calculating the data layers presented here.

References

Baker, C., Thompson, J. R., and Simpson, M.: Hydrological dynamics I: Surface waters, flood and sediment dynamics, in: The Wetlands Handbook, edited by: Maltby, E. and Barker, T., Wiley-Blackwell, Chichester, UK, 120–168, 2009.

Beven, K.: TOPMODEL: a critique, Hydrol. Process., 11, 1069–1085, 1997.

Beven, K.: Rainfall–Runoff Modelling The Primer, 2nd Edn., Wiley-Blackwell, Chichester, UK, 2012.

Beven, K. J. and Cloke, H. L.: Comment on "Hyperresolution global land surface modeling: meeting a grand challenge for monitoring Earth's terrestrial water" by Eric F. Wood et al., Water Resour. Res., 48, W01801, doi:10.1029/2011WR010982, 2012.

Beven, K. J. and Kirkby, M. J.: A physically based, variable contributing area model of basin hydrology, Hydrological Sciences – Bulletin des Sciences Hydrologiques, 24, 43–69, 1979.

Buytaert, W.: Topmodel: implementation of the hydrological model TOPMODEL in R, version 0.7.2–2. R Package, available at: http://cran.r-project.org/web/packages/topmodel/index.html (last access: 6 June 2014), 2011.

Castanho, A. D. A., Coe, M. T., Costa, M. H., Malhi, Y., Galbraith, D., and Quesada, C. A.: Improving simulated Amazon forest biomass and productivity by including spatial variation in biophysical parameters, Biogeosciences, 10, 2255–2272, doi:10.5194/bg-10-2255-2013, 2013.

Chappell, N. A., Vongtanaboon, S., Jiang, Y., and Tangtham, N.: Return-flow prediction and buffer designation in two rainforest headwaters, Forest Ecol. Manag., 224, 131–146, 2006.

Clark, D. B. and Gedney, N.: Representing the effects of subgrid variability of soil moisture on runoff generation in a land surface model, J. Geophys. Res.-Atmos., 113, D10111, doi:10.1029/2007JD008940, 2008.

Coe, M. T.: A linked global model of terrestrial hydrologic processes: simulation of modern rivers, lakes, and wetlands, J. Geophys. Res.-Atmos., 103, 8885–8899, 1998.

Coe, M. T., Costa, M. H., and Soares-Filho, B. S.: The influence of historical and potential future deforestation on the stream flow of the Amazon River – land surface processes and atmospheric feedbacks, J. Hydrol., 369, 165–174, 2009.

Collins, W. J., Bellouin, N., Doutriaux-Boucher, M., Gedney, N., Halloran, P., Hinton, T., Hughes, J., Jones, C. D., Joshi, M., Liddicoat, S., Martin, G., O'Connor, F., Rae, J., Senior, C., Sitch, S., Totterdell, I., Wiltshire, A., and Woodward, S.: Development and evaluation of an

HESSD

11, 6139–6166, 2014

A high-resolution global dataset of topographic index values

T. R. Marthews et al.

Earth-System model – HadGEM2, Geosci. Model Dev., 4, 1051–1075, doi:10.5194/gmd-4-1051-2011, 2011.
Dadson, S. J. and Bell, V. A.: Comparison of Grid-2-Grid and TRIP runoff routing schemes, Report, Centre for Ecology and Hydrology, Wallingford, UK, 2010.
Dadson, S. J., Ashpole, I., Harris, P., Davies, H. N., Clark, D. B., Blyth, E., and Taylor, C. M.: Wetland inundation dynamics in a model of land surface climate: evaluation in the Niger inland delta region, J. Geophys. Res.-Atmos., 115, D23114, doi:10.1029/2010JD014474, 2010.
Dadson, S. J., Bell, V. A., and Jones, R. G.: Evaluation of a grid-based river flow model configured for use in a regional climate model, J. Hydrol., 411, 238–250, 2011.
Dharssi, I., Vidale, P. L., Verhoef, A., Macpherson, B., Jones, C., and Best, M.: New soil physical properties implemented in the Unified Model at PS18, Met Office Technical Report 528, The Met Office, Exeter, UK, 2009.
Ducharne, A.: Reducing scale dependence in TOPMODEL using a dimensionless topographic index, Hydrol. Earth Syst. Sci., 13, 2399–2412, doi:10.5194/hess-13-2399-2009, 2009.
Evans, J.: CT I.aml Compound Topographic Index AML script, available at: http://arcscripts.esri.com/details.asp?dbid=11863 (last access: 6 June 2014) and now part of the Geomorphometry and Gradient Metrics toolbox, available at: http://evansmurphy.wix.com/evansspatial#!arcgis-gradient-metrics-toolbox/crro (last access: 6 June 2014), 2003
Falloon, P. and Betts, R.: Climate impacts on European agriculture and water management in the context of adaptation and mitigation – the importance of an integrated approach, Sci. Total Environ., 408, 5667–5687, 2010.
Open Source Geospatial Foundation: Geospatial Data Abstraction Library (version 1.9.0), Translator library, available at: http://www.gdal.org/ (last access: 6 June 2014), 2011.
Gedney, N. and Cox, P. M.: The sensitivity of global climate model simulations to the representation of soil moisture heterogeneity, J. Hydrometeorol., 4, 1265–1275, 2003.
Gedney, N., Cox, P. M., and Huntingford, C.: Climate feedback from wetland methane emissions, Geophys. Res. Lett., 31, L20503, doi:10.1029/2004GL020919, 2004.
Gedney, N., Cox, P. M., Betts, R. A., Boucher, O., Huntingford, C., and Stott, P. A.: Detection of a direct carbon dioxide effect in continental river runoff records, Nature, 439, 835–838, 2006.

Gerten, D., Schaphoff, S., Haberlandt, U., Lucht, W., and Sitch, S.: Terrestrial vegetation and water balance – hydrological evaluation of a dynamic global vegetation model, J. Hydrol., 286, 249–270, 2004.

Harding, R. J. and Warnaars, T. A.: Water and global change: the WATCH Project Outreach Report, Centre for Ecology and Hydrology, Wallingford, UK, 2011.

Harding, R. J., Blyth, E. M., Tuinenburg, O. A., and Wiltshire, A.: Land atmosphere feedbacks and their role in the water resources of the Ganges basin, Sci. Total Environ., 468, S85–S92, 2013.

Hjerdt, K. N., McDonnell, J. J., Seibert, J., and Rodhe, A.: A new topographic index to quantify downslope controls on local drainage, Water Resour. Res., 40, W05602, doi:10.1029/2004WR003130, 2004.

Intergovernmental Panel on Climate Change: Climate Change 2013: The Physical Science Basis, CUP, Cambridge, UK, 2013.

Junk, W. J., Piedade, M. T. F., Schöngart, J., Cohn-Haft, M., Adeney, J. M., and Wittmann, F.: A classification of major naturally-occurring Amazonian lowland wetlands, Wetlands, 31, 623–640, 2011.

Kirkby, M.: Hydrograph modelling strategies, in: Processes in Physical and Human Geography, edited by: Peel, R., Chisholm, M., and Haggett, P., Heinemann, London, UK, 69–90, 1975.

Lang, M., McCarty, G., Oesterling, R., and Yeo, I.-Y.: Topographic metrics for improved mapping of forested wetlands, Wetlands, 33, 141–155, 2013.

Lehner, B.: HydroSHEDS Technical Documentation (Version 1.2). World Wildlife Fund, Washington, DC, available at: http://hydrosheds.org/page/development (last access: 6 June 2014), 2013.

Lehner, B. and Döll, P.: Development and validation of a global database of lakes, reservoirs and wetlands, J. Hydrol., 296, 1–22, 2004.

Lehner, B. and Grill, G.: Global river hydrography and network routing: baseline data and new approaches to study the world's large river systems, Hydrol. Process., 27, 2171–2186, 2013.

Lehner, B., Verdin, K., and Jarvis, A.: New global hydrography derived from spaceborne elevation data, Eos T. Am. Geophys. Un., 89, 93–94, 2008.

Lewis, S.: Hydrologic Sub-basins of Greenland. Dataset, National Snow and Ice Data Center (NSIDC), Boulder, Colorado, available at: http://nsidc.org/data/nsidc-0371.html (last access: 6 June 2014), 2009.

HESSD

11, 6139–6166, 2014

A high-resolution global dataset of topographic index values

T. R. Marthews et al.

MacKellar, N. C., Dadson, S. J., New, M., and Wolski, P.: Evaluation of the JULES land surface model in simulating catchment hydrology in Southern Africa, Hydrol. Earth Syst. Sci. Discuss., 10, 11093–11128, doi:10.5194/hessd-10-11093-2013, 2013.

Marthews, T. R., Malhi, Y., Girardin, C. A. J., Silva-Espejo, J. E., Aragão, L. E. O. C., Metcalfe, D. B., Rapp, J. M., Mercado, L. M., Fisher, R. A., Galbraith, D. R., Fisher, J. B., Salinas-Revilla, N., Friend, A. D., and Restrepo-Coupe, N.: Simulating forest productivity along a neotropical elevational transect: temperature variation and carbon use efficiency, Global Change Biol., 18, 2882–2898, 2012.

Marthews, T. R., Quesada, C. A., Galbraith, D. R., Malhi, Y., Mullins, C. E., Hodnett, M. G., and Dharssi, I.: High-resolution hydraulic parameter maps for surface soils in tropical South America, Geosci. Model Dev., 7, 711–723, doi:10.5194/gmd-7-711-2014, 2014.

Milly, P. C. D., Betancourt, J., Falkenmark, M., Hirsch, R. M., Kundzewicz, Z. W., Lettenmaier, D. P., and Stouffer, R. J.: Stationarity is dead: whither water management?, Science, 319, 573–574, 2008.

Moore, I. D., Lewis, A., and Gallant, J. C.: Terrain attributes: estimation methods and scale effects, in: Modelling Change in Environmental Systems, edited by: Jakeman, A. J., Beck, M. B., and McAleer, M. J., John Wiley and Sons Ltd., Chichester, UK, 189–214, 1993.

O'Connor, F. M., Boucher, O., Gedney, N., Jones, C. D., Folberth, G. A., Coppell, R., Friedlingstein, P., Collins, W. J., Chappellaz, J., Ridley, J., and Johnson, C. E.: Possible role of wetlands, permafrost, and methane hydrates in the methane cycle under future climate change: a review, Rev. Geophys., 48, RG4005, doi:10.1029/2010RG000326, 2010.

Pangala, S. R., Moore, S., Hornibrook, E. R. C., and Gauci, V.: Trees are major conduits for methane egress from tropical forested wetlands, New Phytol., 197, 524–531, 2013.

Pfeffer, W. T., Arendt, A. A., Bliss, A., Bolch, T., Cogley, J. G., Gardner, A. S., Hagen, J.-O., Hock, R., Kaser, G., Kienholz, C., Miles, E. S., Moholdt, G., Mölg, N., Paul, F., Radić, V., Rastner, P., Raup, B. H., Rich, J., Sharp, M. J., and The Randolph Consortium: The Randolph Glacier Inventory: a globally complete inventory of glaciers, J. Glaciol., 60, 537–552, 2014.

Prentice, I. C., Bondeau, A., Cramer, W., Harrison, S. P., Hickler, T., Lucht, W., Sitch, S., Smith, B., and Sykes, M. T.: Dynamic global vegetation modeling: quantifying terrestrial ecosystem responses to large-scale environmental change, in: Terrestrial Ecosystems in a Changing World, edited by: Canadell, J. G., Pataki, D. E., and Pitelka, L. F., Springer, Berlin, Germany, 175–192, 2007.

Prigent, C., Papa, F., Aires, F., Rossow, W. B., and Matthews, E.: Global inundation dynamics inferred from multiple satellite observations, 1993–2000, J. Geophys. Res., 112, D12107, doi:10.1029/2006JD007847, 2007.

Quinn, P., Beven, K., Chevallier, P., and Planchon, O.: The prediction of hillslope flow paths for distributed hydrological modelling using digital terrain models, Hydrol. Process., 5, 59–79, 1991.

Quinn, P. F., Beven, K. J., and Lamb, R.: The ln($a/\tan\beta$) index: how to calculate it and how to use it within the TOPMODEL frameworkm, Hydrol. Process., 9, 161–182, 1995.

R Development Core Team: R: A language and environment for statistical computing, version 3.0.2. R Foundation for Statistical Computing, Vienna, available at: http://www.R-project.org (last access: 6 June 2014), 2013.

Sanderson, M. G., Wiltshire, A. J., and Betts, R. A.: Projected changes in water availability in the United Kingdom, Water Resour. Res., 48, W08512, doi:10.1029/2012WR011881, 2012.

Seneviratne, S. I., Lüthi, D., Litschi, M., and Schär, C.: Land–atmosphere coupling and climate change in Europe, Nature, 443, 205–209, 2006.

Seneviratne, S. I., Corti, T., Davin, E. L., Hirschi, M., Jaeger, E. B., Lehner, I., Orlowsky, B., and Teuling, A. J.: Investigating soil moisture–climate interactions in a changing climate: a review, Earth-Sci. Rev., 99, 125–161, 2010.

US Geological Survey: HYDRO1k Elevation derivative database, US Geological Survey Earth Resources Observation and Science (EROS) Center, Sioux Falls, South Dakota, available at: https://lta.cr.usgs.gov/HYDRO1K (last access: 6 June 2014) downloaded from EarthExplorer 18 October 2013, 2000.

Wainwright, J. and Mulligan, M.: Environmental Modelling Finding Simplicity in Complexity, 2nd Edn, Wiley-Blackwell, Chichester, UK, 2013.

Ward, R. C. and Robinson, M.: Principles of Hydrology, 4th edn., McGraw-Hill, Maidenhead, UK, 2000.

Wilson, J. P. and Gallant, J. C.: Terrain Analysis Principles and Applications, John Wiley and Sons, New York, 2000.

Wolock, D. M. and McCabe, G. J.: Comparison of single and multiple flow direction algorithms for computing topographic parameters in TOPMODEL, Water Resour. Res., 31, 1315–1324, 1995.

Wood, E. F., Roundy, J. K., Troy, T. J., van Beek, L. P. H., Bierkens, M. F. P., Blyth, E., de Roo, A., Döll, P., Ek, M., Famiglietti, J., Gochis, D., van de Giesen, N., Houser, P.,

HESSD

11, 6139–6166, 2014

A high-resolution global dataset of topographic index values

T. R. Marthews et al.

Jaffé, P. R., Kollet, S., Lehner, B., Lettenmaier, D. P., Peters-Lidard, C., Sivapalan, M., Sheffield, J., Wade, A., and Whitehead, P.: Hyperresolution global land surface modeling: meeting a grand challenge for monitoring Earth's terrestrial water, Water Resour. Res., 47, W05301, doi:10.1029/2010WR010090, 2011.

Wood, E. F., Roundy, J. K., Troy, T. J., van Beek, R., Bierkens, M., Blyth, E., de Roo, A., Döll, P., Ek, M., Famiglietti, J., Gochis, D., van de Giesen, N., Houser, P., Jaffe, P., Kollet, S., Lehner, B., Lettenmaier, D. P., Peters-Lidard, C. D., Sivapalan, M., Sheffield, J., Wade, A. J., and Whitehead, P.: Reply to comment by Keith J. Beven and Hannah L. Cloke on "Hyperresolution global land surface modeling: meeting a grand challenge for monitoring Earth's terrestrial water", Water Resour. Res., 48, W01802, doi:10.1029/2011WR011202, 2012.

Zhao, G., Gao, J., Tian, P., and Tian, K.: Comparison of two different methods for determining flow direction in catchment hydrological modeling, Water Sci. Eng., 2, 1–15, 2009.

Zulkafli, Z., Buytaert, W., Onof, C., Lavado, W., and Guyot, J. L.: A critical assessment of the JULES land surface model hydrology for humid tropical environments, Hydrol. Earth Syst. Sci., 17, 1113–1132, doi:10.5194/hess-17-1113-2013, 2013.

Table 1. Topographic index values from the *GA2* algorithm applied to *HydroSHEDS* data (Appendix A) compared to CTI values from HYDRO1k for all global river basins larger than 10^6 km^2. Note that some sources quote much higher index values, but these are often not scale-corrected values and are therefore not directly comparable (e.g. Yang et al., 2007).

River catchments	Area[a] (million km^2)	CTI of HYDRO1k **Mean**	SD	Min	Max	GA2 based on HydroSHEDS **Mean**	SD	Min	Max	Percentage increase moving from CTI to GA2
Africa										
Congo	3.70 (0.04)	**6.98**	2.20	0.87	23.24	**5.97**	2.42	0.98	24.54	−14.5
Nile	3.40 (0.07)	**6.69**	2.39	0.61	23.29	**6.74**	2.53	0.49	24.23	+0.7
Niger	2.12 (0.00)	**7.27**	2.20	0.94	22.78	**6.72**	2.36	0.75	23.97	−7.6
Zambezi	1.39 (0.03)	**6.34**	2.24	0.47	21.25	**6.41**	2.43	0.64	23.42	+1.1
Asia										
Ob-Irtysh	2.97 (0.02)	**6.60**	2.06	0.64	22.2	**6.70**	2.41	0.06	24.58	+1.5
Yenisei	2.58 (0.07)	**4.93**	2.06	0.57	22.95	**5.20**	2.50	0.00	24.22	+5.5
Lena	2.50 (0.00)	**4.91**	1.98	0.73	22.57	**5.20**	2.51	0.00	24.34	+5.9
Amur/Heilong Jiang	1.86 (0.02)	**5.24**	2.11	0.84	21.8	**5.47**	2.73	0.74	24.18	+4.4
Yangtze/Chang Jiang	1.81 (0.01)	**4.56**	2.33	0.04	21.63	**4.55**	2.75	0.00	23.86	−0.2
Indus	1.17 (0.03)	**5.55**	2.85	0.00	21.56	**5.71**	3.03	0.01	22.98	+2.9
Ganges	1.08 (0.01)	**6.38**	2.61	0.05	21.81	**6.43**	2.81	0.00	23.22	+0.8
Mekong	0.80 (0.00)	**5.29**	2.50	0.54	22.01	**5.39**	2.85	0.53	22.98	+1.9
Yellow/Huang He	0.75 (0.00)	**5.25**	2.26	0.73	21.68	**5.42**	2.74	0.54	23.01	+3.2
Australasia										
Murray-Darling	1.06 (0.00)	–[b]	–[b]	–[b]	–[b]	**6.94**	2.44	1.01	22.73	–[b]
Europe										
Volga	1.38 (0.03)	**6.35**	2.05	1.30	22.61	**6.21**	2.33	1.11	23.74	−2.2
Danube	0.82 (0.00)	**5.44**	2.45	0.51	21.42	**5.44**	2.80	0.16	23.16	+0.0
Rhine	0.17 (0.00)	**5.52**	2.31	0.52	19.79	**5.36**	2.64	0.09	21.64	−2.9
North America										
Mississippi-Missouri	2.98 (0.02)	**6.21**	2.02	0.80	22.57	**6.16**	2.47	0.47	24.46	−0.8
Mackenzie	1.81 (0.17)	**6.09**	2.53	0.56	22.57	**6.11**	2.56	0.00	24.24	+0.3
St. Lawrence	1.34 (0.30)	**7.33**	2.74	1.33	21.49	**6.10**	2.36	0.91	23.46	−16.8
Nelson-Saskatchewan	0.89 (0.09)	**7.16**	2.13	0.69	21.43	**6.76**	2.31	0.06	23.52	−5.6
South America										
Amazon	7.05 (0.01)	**7.67**	2.42	0.00	23.99	**6.11**	2.54	0.42	25.00	−20.3
Paraná (excl. Río de la Plata)	2.58 (0.02)	**7.13**	2.27	0.56	23.27	**6.44**	2.62	0.54	24.26	−9.7
Orinoco	0.88 (0.00)	**6.74**	2.27	0.31	22.19	**6.28**	2.65	0.38	23.15	−6.8

[a] Area of lakes, reservoirs, glaciers and ice sheets within the basin given in parentheses (the topographic index is not evaluated at these pixels by GA2, whereas the HYDRO1k CTI calculation assigns values to lakes as if they are flat plains, Appendix A).
[b] HYDRO1k did not include mainland Australia therefore no CTI values are available for the Murray-Darling (USGS, 2000).

HESSD
11, 6139–6166, 2014

Table 2. Topographic index values from the GA2 algorithm applied to HydroSHEDS data (Appendix A). For a map of the extent of these wetland types, see Lehner and Döll (2004).

Wetland type[a]	Area[b] (million km^2)	Topographic index (dimensionless)			
		Mean value	SD	Min	Max
Ice-free land outside wetlands and wetland complexes	128.99	5.88	2.56	0.00	24.69
Intermittent Wetlands/Lakes (mostly in drylands)	0.66	8.07	2.89	0.59	24.03
Pans, Brackish/Saline Wetlands (mostly temperate and subtropical)	0.40	7.91	2.59	0.82	23.09
Freshwater Marsh, Floodplains	2.72	7.38	2.45	0.56	24.89
Mires (e.g. bogs, fens) (mostly boreal)	1.23	5.97	2.56	0.00	24.06
Swamp Forests, Inundated Forests (mostly S. America and Congo)	0.94	6.92	2.48	0.86	25.00
Coastal Wetlands (e.g. mangroves, estuaries, deltas, lagoons)	0.45	7.03	2.22	0.58	24.54
River pixels	0.42	8.81	4.80	0.16	25.00
Wetland Complex (0–25 % wetland) (Asia only, mostly India and Tibetan China)	0.83	5.61	2.52	0.30	22.28
25–50 % wetland (USA and Canada only)	4.01	6.47	2.30	0.09	24.33
50–100 % wetland (USA and Canada only)	2.76	6.84	2.38	0.00	24.45

[a] Following the high-resolution Global Lakes and Wetlands Database (*GLWD*, Lehner and Döll, 2004).
[b] These areas sum to 143.43×10^6 km^2 which is the global extent of land not covered by lakes, reservoirs, glaciers or ice sheets that lies outside Antarctica and other islands excluded from *HydroSHEDS* (*viz.* Antarctica, Polynesia east of the 180° meridian line, the Azores, St Helena, Ascension Is., Tristan da Cunha, South Georgia, the South Sandwich Is., the Kerguelen Archipelago and some smaller oceanic islands, Lehner et al., 2008). Permanent lakes and reservoirs cover 1.23×10^6 km^2 globally (Lehner and Döll, 2004), the Greenland ice sheet covers 1.99×10^6 km^2 (Lewis, 2009) and all glaciers cover 0.80×10^6 km^2 (Pfeffer et al., 2014).

HESSD
11, 6139–6166, 2014

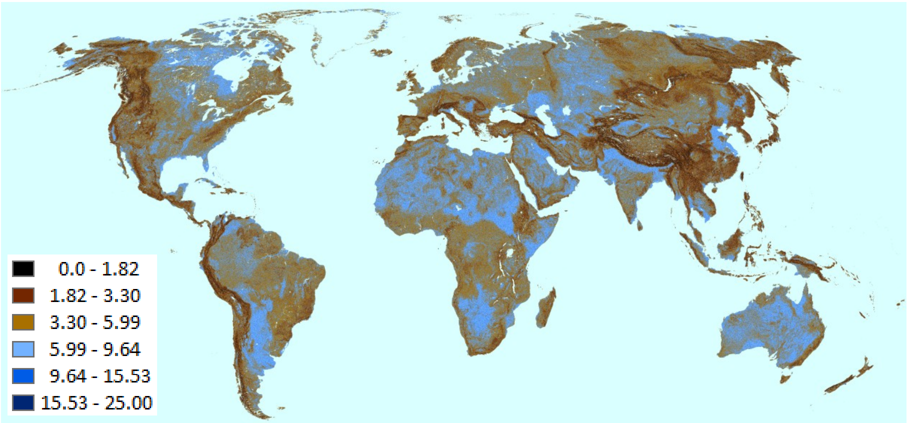

Figure 1. Global topographic index values based on *GA2* appplied to *HydroSHEDS* base data (Appendix A). Blue shades indicate pixels with index values above the global mean (5.99) and brown shades indicate below-average values.

HESSD
11, 6139–6166, 2014

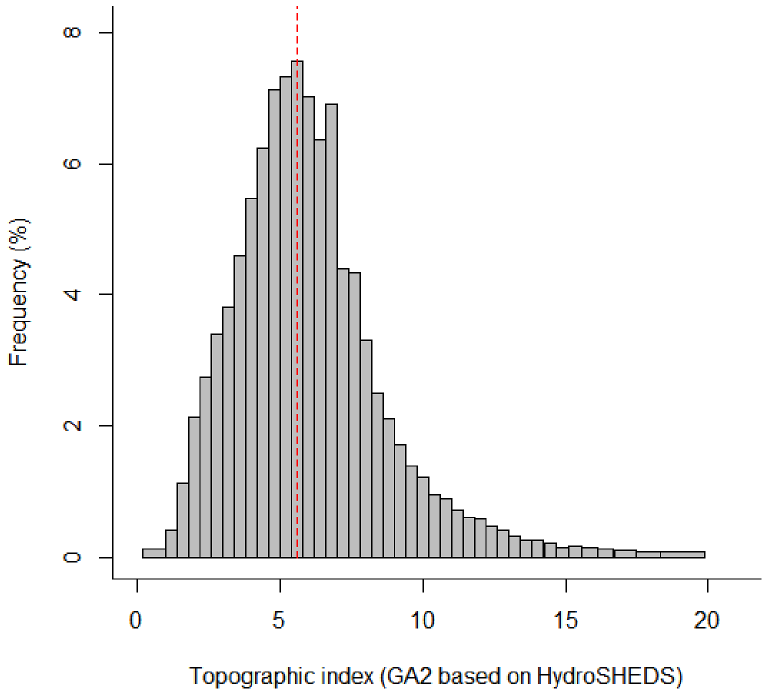

Figure 2. Histogram of global topographic index values (vertical line shows global mean of 5.99; global maximum is 25.0044 at a pixel within a river island at the confluence of the Amazon and Xingú rivers in Brazil).

HESSD
11, 6139–6166, 2014

Figure 3. Comparison of topographic index calculations, divided by wetland type (following Lehner and Döll, 2004, excluding lakes and reservoirs): TI (dark shaded box) = calculations of topographic index from this study (also shown as a horizontal solid line; precise figures given in Table 2), and H1k (light shaded box) = the Compound Topographic Index of HYDRO1k (USGS, 2000), both of which applied the scale-correction of Ducharne (2009). Boxes show mean ± SD index values for the global distribution of that wetland type. For reference, the mean topographic index value for ice-free land outside wetlands is shown by a broken line on all panels (Table 2).

HESSD
11, 6139–6166, 2014

A high-resolution global dataset of topographic index values

T. R. Marthews et al.

Title Page
Abstract | Introduction
Conclusions | References
Tables | Figures
◀I | ▶I
◀ | ▶
Back | Close
Full Screen / Esc
Printer-friendly Version
Interactive Discussion

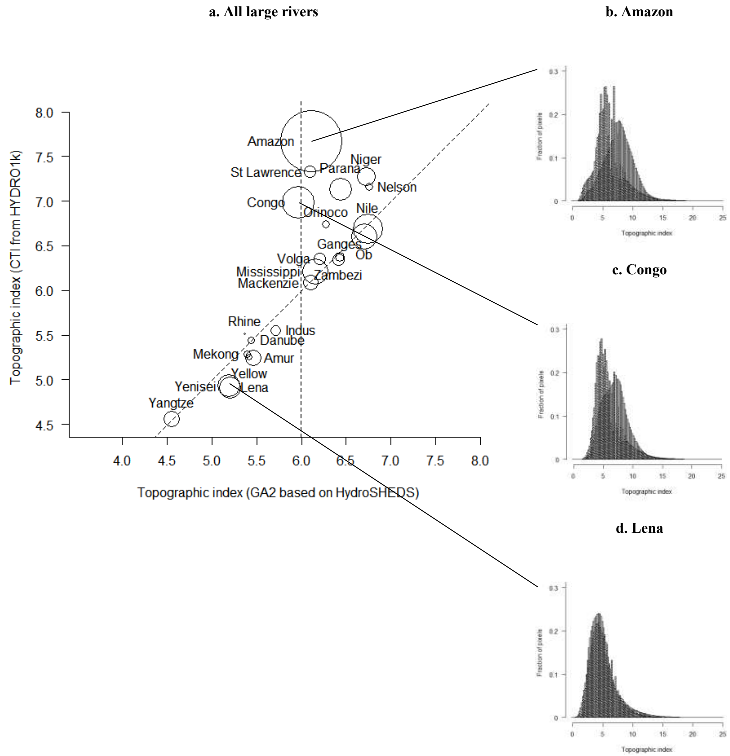

Figure 4. Comparison of the CTI and *GA2* calculations of the topographic index (from Table 1), showing that CTI values are larger for some catchments, most notably the Amazon, Congo, Paraná, Niger and St. Lawrence. A one-one line is shown for reference and circle areas are proportional to catchment area. The largest catchments tend to be closest to the global average index value of 5.99 (also shown for reference). Histograms are shown for three catchments: Amazon, Congo and Lena (each grey histogram shows CTI values, hatched histogram shows *GA2*): for catchments close to the one-one line, the corresponding histograms were closely similar.

HESSD
11, 6139–6166, 2014

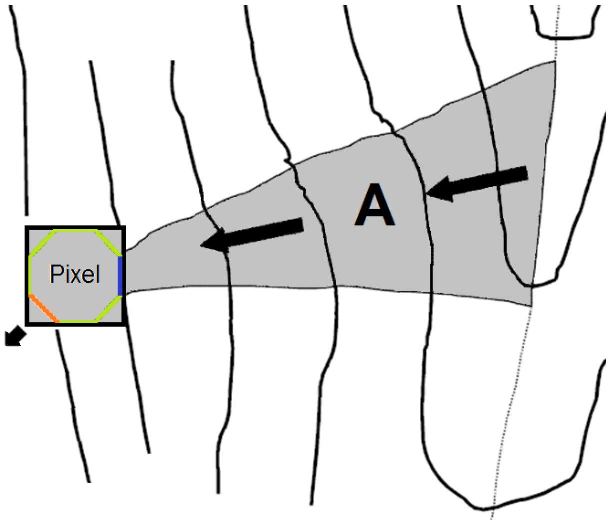

Figure A1. Illustration of the topographic index calculation of *GA2* for one pixel of a *DEM* (the black square) downstream from a catchment area A (in m^2, defined to include the area of the pixel itself, which is usually negligible in comparison to A). The *inflow contour* of the pixel is shown in blue, the *outflow contour* in orange and the remaining perimeter of the octagon is shown green (q.v. the octagon of contour lengths shown in Quinn et al., 1991, Fig. 1). We calculate DX = (pixel sidelength in m), $\tan(\beta)$ = (mean slope across the outflow contour), $\tan(\beta')$ = (mean slope across the non-outflow contour (blue+green)), clout = (outflow contour length in m), a = (specific catchment area in m) = A/clout (n.b. called an "area" but units are $m^2\,m^{-1}$ = m) and dfltsink = $\ln\left(\frac{A}{2DX\tan(\beta')}\right)$ (this default value for *sinks*, i.e. pixels with no outflow, is described in Quinn et al., 1995, Fig. 14). The **topographic index value for this cell** is defined as $\ln\left(\frac{a}{\tan(\beta)}\right)$ if clout $\neq 0$ or = dfltsink if clout = 0 (Quinn et al., 1991, 1995).

HESSD
11, 6139–6166, 2014

Title Page
Abstract Introduction
Conclusions References
Tables Figures
◀| |▶
◀ ▶
Back Close
Full Screen / Esc
Printer-friendly Version
Interactive Discussion